

Article

Research on the Accumulated Plastic Strain of Expansive Soil under Subway Loading

Lei Zhu ¹, Ying Guo ², Gan Cheng ^{1,*} and Xiangyang Liu ¹

¹ School of Urban Construction and Transportation, Hefei University, Hefei 230601, China; zhuleianhui@163.com (L.Z.); lxymm9632@163.com (X.L.)

² School of Civil Engineering, Anhui Jianzhu University, Heifei 230601, China; guoying626@std.ahjzu.edu.cn

* Correspondence: chenggan0713@163.com

Abstract: Expansive soil near Hefei Xinqiao International Airport was selected as the research focus. The effects of different loading modes on the dynamic strain of the saturated remodeled expansive soil was investigated by indoor dynamic triaxial tests and the effect of three factors, intermittent loading ratio, static deviatoric stress, and cyclic stress ratio, on the accumulated plastic strain of saturated remodeled expansive soil under intermittent subway cyclic loading was analyzed. Finally, the corresponding accumulated plastic strain calculation model was established based on the test results. The research results show that the loading modes do not affect the overall development mode of the strain and, under intermittent loading, the strain tends to be more stable. Under intermittent loading, when the number of cycles is the same, the larger the intermittent loading ratio, the smaller the accumulated plastic strain. The effect of static deviatoric stress and cyclic stress ratio on strain accumulation is significant. Based on the hyperbolic model, an accumulated plastic strain calculation model related to the number of cycles of remolded expansive soil under the load of the Hefei subway was proposed, which has a certain reference significance for the design, safety assessment, and safe operation of the Hefei subway.

Keywords: subway loads; expansive soil; dynamic strain; accumulated plastic strain model



Citation: Zhu, L.; Guo, Y.; Cheng, G.; Liu, X. Research on the Accumulated Plastic Strain of Expansive Soil under Subway Loading. *Appl. Sci.* **2023**, *13*, 9994. <https://doi.org/10.3390/app13189994>

Academic Editors: Xianwei Zhang, Xinyu Liu and Ran An

Received: 10 August 2023

Revised: 24 August 2023

Accepted: 29 August 2023

Published: 5 September 2023



Copyright: © 2023 by the authors. Licensee MDPI, Basel, Switzerland. This article is an open access article distributed under the terms and conditions of the Creative Commons Attribution (CC BY) license (<https://creativecommons.org/licenses/by/4.0/>).

1. Introduction

Expansive soil is widely distributed throughout the world and is known to exist in more than forty countries on six continents, of which China is one of the countries with the widest distribution and largest area of expansive soil [1,2]. Although these countries are geographically different and have different climatic environments, they all face the same problem of expansive soil hazards. Expansive soil poses formidable challenges in engineering construction and operational safety. Highways and railways constructed in expansive soil regions become “roadblocks” and “hard nuts” to crack. They epitomize the saying “Where there is a ditch, there is a slip; where there is a dike, there is a collapse”. Similarly, working with river channels in these areas is akin to “Digging a foot during the day, only to find it stretches eight feet longer at night”. Expansive soil not only causes great obstruction to above-ground projects such as buildings, highways, railroads, and canal slopes, but also poses a serious threat to underground engineering projects such as underground railways, pipelines, tunnels, and foundation structures [3–5]. The repetitive nature, complexity, and long-term potential hazards are hallmark features of expansive soil disasters, posing persistent challenges to the engineering community. The magnitude and widespread impact of the damages resulting from the unfavorable properties of expansive soil often necessitate significant human, material, and financial resources to address this unique geological hazard. According to statistics, the United States allocates billions of dollars each year towards addressing the issue of expansive soil hazards, surpassing the cumulative losses from disasters such as floods, hurricanes, earthquakes, and tornadoes.

Likewise, in China, the economic losses caused by expansive soil amount to over billions of dollars annually [6]. Hence, expansive soil has been recognized as a “cancer” that impedes engineering construction globally.

So far, researchers have made significant strides in studying the composition of expansive soil minerals, their macro–micro structure, swelling–shrinkage mechanisms, and physical–mechanical properties. However, there remains a relative scarcity of research concerning the mechanical properties of expansive soil under dynamic loading conditions.

Tang et al., investigated the attenuation patterns of a dynamic elastic modulus of saturated expansive soil under various influencing factors. Based on this, they established a model for the attenuation of a dynamic elastic modulus related to compaction degree, reinforcement layers, confining pressure, and frequency [7]. Yang et al., examined the dynamic shear modulus and damping ratio of expansive soil under freeze–thaw conditions. The results indicated that freeze–thaw cycles led to an increase in the dynamic elastic modulus of expansive soil, but a decrease in the damping ratio [8]. These researchers explored different experimental conditions to study dynamic modulus indices of expansive soil under dynamic loading. However, it is worth noting that under lower dynamic loads, the soil exhibits elastic deformation with closed hysteresis loops. In this scenario, dynamic shear modulus or dynamic elastic modulus can effectively describe the soil’s ability to resist dynamic elastic deformation. Yet, under higher dynamic loads, the soil experiences irreversible strains, and hysteresis loops no longer close. Consequently, dynamic shear modulus or dynamic elastic modulus lose their significance.

Considering this, Chen and Zhang investigated the changing patterns of accumulated plastic strain under significant dynamic loading on expansive soil, proposing a corresponding strain model to predict strain growth during prolonged cyclic loading [9,10]. However, their simulation of dynamic loading in indoor experiments lacked meticulous detailing or a comprehensive rationale for employing sine wave simulation of dynamic loading.

In summary, the research on the strain development patterns of expansive soil under dynamic loading is still relatively limited, and a comprehensive and scientifically grounded theory has yet to be established. Furthermore, due to variations in soil properties across different regions, research outcomes also exhibit disparities. Therefore, this study employs indoor dynamic triaxial tests to investigate the impact of various factors on the strain behavior of expansive soil in the Hefei region under subway loading. The dynamic loading in the experiments is designed to closely emulate the authentic characteristics of subway loading to the greatest extent possible.

2. Dynamic Triaxial Test Plan

2.1. Test Equipment

The dynamic triaxial testing was performed utilizing the sophisticated electric motor-controlled dynamic triaxial testing system (DYNTTS) produced by GDS Company in the United Kingdom, as shown in Figure 1. The DYNTTS system finds extensive application in indoor experimental research on the dynamic properties of geotechnical materials. It not only facilitates dynamic testing of soils but also seamlessly integrates the entire suite of testing capabilities offered by static triaxial testing instruments. This system enables the execution of a range of experiments, such as soil sample consolidation, saturation, and dynamic loading tests. Moreover, during the testing process, it provides real-time dynamic visualization of experimental data.

2.2. Test Soil Samples and Remolded Soil Sample Preparation

The test soil was extracted from the expansive soil samples located near the subway station of Xinqiao International Airport in Hefei City. The diameter of the soil samples was 80 mm and the height was 200 mm, as shown in Figure 2.



Figure 1. Dynamic triaxial testing system (DYNTTS).

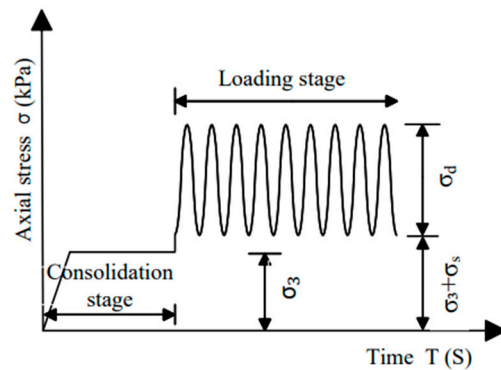


Figure 2. Schematic diagram of continuous cyclic loading waveform in the dynamic triaxial test.

The test soil was collected from the expansive soil at a subway station near Hefei Xinqiao International Airport in Hefei City. The soil samples were obtained with a diameter of 80 mm and a height of 200 mm. The retrieved soil samples of expansive soil were first subjected to a series of physical property index tests, with the experimental operations based on the “Geotechnical Testing Methods Standard” (GB/T50123-2019) [11]. The basic physical property indices of the undisturbed expansive soil samples are shown in Table 1, and according to the “Technical Code for Construction of Expansive Soil Areas” (GB 50112-2013) [12], the free swell ratio of the undisturbed soil samples falls within the range of 65% to 90%, therefore, the tested soil can be classified as moderately expansive.

Table 1. Basic physical property indices of soil samples.

ω (%)	ρ (g·cm ⁻³)	W_L (%)	W_P (%)	I_p	δ_{ef} (%)
21.40	1.74	48.82	29.19	19.63	68

To ensure the uniformity of the soil texture and prevent the influence of physical parameter variations on the experiments, it was necessary to control other parameters and maintain consistency. Therefore, a series of studies was conducted using saturated remolded soil samples. The specific procedures for preparing the samples are as follows: (1) remove the soil sample from the sampling cylinder and cut it into slices, placing them on a tray. Then, put the tray into the drying oven and dry the soil at 110 °C for 24 h to ensure complete desiccation. (2) Crush and sieve the dried sample manually and mechanically, leaving soil particles with a diameter ranging from 1 mm to 2 mm. Then, thoroughly mix

the sieved soil and measure the moisture content of the sample. (3) Utilize the wet method for sample preparation. Calculate the mass and moisture content of the dry soil required for the experiment based on the predetermined moisture content and maximum dry density. Add water to the dry soil container to reach the required moisture content. Additionally, cover the surface of the container with a damp cloth and allow it to rest undisturbed for 12 h to ensure uniform moisture distribution within the soil material. (4) Following the completion of wet soil sample preparation, employ a compaction method to compact the soil sample. Weigh the designated sample quantity, then pour it into the compaction mold in seven layers, ensuring an even distribution and leveling the soil surface. Throughout the testing process, it is essential to maintain consistent layer heights, and the layered surfaces should undergo trimming to remove excess soil. (5) Once the compaction is finished, use a cutting ring to extract a soil sample for weighing. Measure the moisture content of the soil samples cut from both ends of the ring, with an acceptable error range of $\pm 1\%$. After completing the sample preparation, wrap it with cling film and allow it to rest undisturbed in preparation for the dynamic triaxial test.

2.3. Experimental Parameter Settings

The experimental conditions are crucial factors that impact the dynamic characteristics of the soil. To conduct this experiment reasonably, it is essential to make informed choices based on the research objectives and content, aiming to closely align with the actual field conditions and faithfully replicate the real-life scenario. The specific configuration of experimental parameters and conditions includes determining the influential factors of the experiment, establishing the parameters relevant to subway loading, and considering other control conditions for the experiment.

2.3.1. Determination of Experimental Influencing Factors

In general, the main influencing factors of the dynamic characteristics of expansive soil can be divided into two aspects: firstly, from the perspective of dynamic loads, factors such as the load waveform, stress amplitude, vibration frequency, and duration of action are crucial. Secondly, in relation to the experimental soil sample, factors mainly include the consolidation state of the soil (consolidation ratio, overconsolidation ratio) and the stress state of the soil (confining pressure, initial force conditions, etc.). Based on the research background and objectives of this paper, the experimental investigation focuses on three key factors as the influencing parameters: the intermittent loading ratio, the static deviatoric stress, and the cyclic stress ratio. The specific parameter settings are shown below.

(1) Intermittent Loading Ratio

Considering the intermittent nature of subway loading, the intermittent loading ratio is defined as the ratio of the intermittent loading duration ΔT and the functioning time of the subway loading T . The specific parameter settings for the intermittent loading ratio are determined as follows: since the typical subway train in Hefei City consists of six sections of Type B drum-shaped cars, with a length of approximately 120 m, and the train speed ranges from 30 to 80 km/h, the time taken for the subway to pass a specific point can be calculated as 5.4 s to 14.4 s. Taking 10 s as the time for the subway to pass a specific point, the intermittent duration is generally tens of times the running time [13]. The selected values for the intermittent loading ratio $\Delta T/T$ are 1, 5, 10, and 50, thus corresponding to intermittent durations of 10 s, 50 s, 100 s, and 500 s. A control experiment is also included with $\Delta T/T = 0$.

(2) Static Deviatoric Stress

The real loads imposed on the soil under train loading include a static load and cyclic dynamic loads, where the static load is caused by the instantaneous bias stress applied to the soil by the passing train. Researchers such as Wen et al. [14] have studied the effect of static deviatoric stress ratio on the deformation behavior of saturated clay. The loading procedure is as follows: a specific static deviator stress is first applied to a predetermined

value, and then sinusoidal cyclic loads are superimposed on this static deviator stress. In the experiment, the static deviatoric stress ratios are set to 0, 0.1, and 0.2, with an effective consolidated confining pressure of 100 kPa. The results show that an increase in static deviator stress is detrimental to soil stability, and higher static deviator stress results in greater soil deformation. Similar experimental results were obtained by Chen et al. [15] and Wang et al. [16] regarding the influence of static deviator stress.

In addition, it has been found that the existence of static deviatoric stress may also cause preloading of the soil, which may increase the strength of the soil. Furthermore, the method of loading can impact the experimental outcomes, making it necessary to further study the influence of static deviator stress as a contributing factor. According to previous research results [17], the instantaneous stress produced by the tunnel surrounding soil under subway trains operation is 20~40 kPa. Chen et al. [18] considered the static load effects of the overlying structure (ballast, track, and rail sleeper) and used a static deviatoric stress of 15 kPa. In this paper, two different static deviatoric stresses of 15 kPa and 30 kPa are selected for comparison and analysis.

(3) Cyclic Stress Ratio

As one of the most important factors affecting the dynamic characteristics of soil, cyclic stress ratio can not be ignored in triaxial dynamic tests. The cyclic stress ratio η_d is defined as the ratio of the dynamic load amplitude (the difference between the peak and trough of the load) σ_d to the confining pressure σ_c . In the experiment, cyclic stress ratios η_d of 0.1, 0.2, and 0.4 were set.

2.3.2. Determination of Parameters Related to Subway Loads

(1) Load Waveform

Previous scholars have demonstrated that the subway running load has obvious characteristics of harmonic waves, and among various waveforms, the biased sinusoidal waveform closely approximates the actual subway train load. It can not only simulate the instantaneous bias stress generated by the train passing through the soil, but also meet the requirement that the soil experiences only compressive stress under subway loading conditions. Therefore, the biased sinusoidal wave is selected as the subway load waveform, as depicted in Figures 2 and 3.

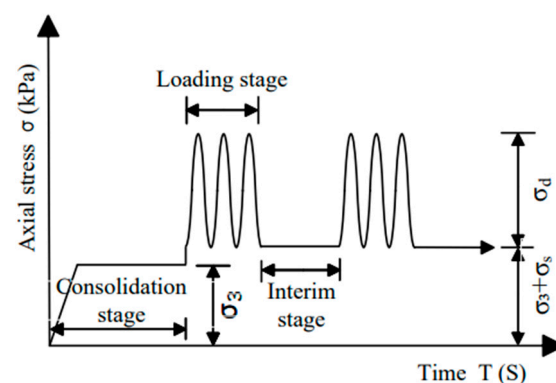


Figure 3. Schematic diagram of intermittent cyclic loading waveform in the dynamic triaxial test.

(2) Vibration Frequency

Zhang Yu'e [19] proposed that the main vibration caused by passing subway trains is of low frequency, and the high-frequency vibration has a minimal impact on structures. Based on research, Lei Shengyou et al. [20] found that the frequency of dynamic loads has little effect on the deformation of expansive soil. Zhou Xiaosheng [21] conducted experimental research on remolded expansive soil, and reached the conclusion that there is no significant regular change in the dynamic strain, dynamic elastic modulus, and damping ratio of the soil when the frequencies are 1 Hz and 2 Hz. Zhuang Jiahua [22] determined

the frequency of cyclic loading as 1 Hz based on measured data. Therefore, the influence of frequency on the dynamic loading tests for expansive soil is no longer considered, and a uniform value of 1 Hz is adopted.

2.3.3. Other Experimental Control Conditions

(1) Soil Consolidation Conditions

The actual consolidation state of the soil sample is not isotropic consolidation but is in a biased consolidation state. Therefore, the test adopts the biased consolidation condition of the soil, using the K_0 consolidation module provided by GDS, with an effective confining pressure of 120 kPa.

(2) Drainage Conditions and Test Termination Conditions

Both drained and undrained conditions are considered for the intermittent loading conditions of the subway, whereas only the undrained conditions are used for the continuous loading conditions of the subway.

The termination conditions for the continuous loading test are either when the axial strain reaches 10% or when the total number of cycles reaches 10,000, with the damage condition when the axial strain reaches 5%. For the intermittent loading test, the applied loads are relatively small, resulting in small strains ranging from 10^{-3} to 10^{-2} . The dynamic triaxial tests are performed with intermittent durations ranging from 10 s to 500 s. The instrument cannot automatically perform the cyclic loading and unloading operations, prolonged repeated loading and unloading following the termination condition for continuous loading can cause damage to the machine. Therefore, the termination condition for non-continuous loading tests are different from those for continuous loading tests. When the strain stabilizes within a certain range (order of magnitude 10^{-4}), the test is terminated, and the same number of cycles is controlled to avoid test errors caused by long-term manual operation.

In summary, the test scheme is shown in Table 2.

Table 2. Dynamic triaxial test plan.

Sample ID	Loading Method	Loading Time T (s)	Intermission Time ΔT (s)	Intermittent Loading Ratio $\Delta T/T$	Static Deviatoric Stress σ_s (kPa)	Cyclic Stress Ratio η_d
S1~S6	Continuous Loading	-	-	-	15	0.1
S7~S12			10	1		
S13~S18	Intermittent Loading	10	50	5	30	0.2
S19~S24			100	10		
S25~S30			500	50		

3. Analysis of Test Results

3.1. Analysis of the Influence Law of Loading Methods on the Dynamic Strain of Expansive Soil

Figure 4a shows the dynamic strain–time curve of sample S3 under continuous loading conditions, while Figure 5a shows the dynamic strain–time curve of sample S21 under intermittent loading conditions (first 800 s). It can be observed from the figures that both loading modes exhibit dynamic strains comprising elastic strain ε_p and accumulated plastic strain ε_d . Unlike continuous loading, the dynamic strain–time curve under intermittent loading conditions develops in a “step-like” manner, including loading and intermittent phases. The strain value during the loading phase increases with time, while the strain value during the intermittent phase remains close to the strain value at the end of the loading phase, with a “strain platform” existing between the two phases. During each cycle, the strain experiences a period of growth followed by a period of nearly constant values. The reason for this is that under partially drained conditions, the axial strain is mainly composed of two parts: one is the volume change caused by the drainage of pore

water, which leads to a decrease in the total volume of the soil sample and a corresponding decrease in the pore size between soil particles; the other is the deformation of the soil sample due to external loads. However, the deformation of the soil caused by the discharge of pore water accounts for the majority of the deformation. In addition, because the intermittent period stops loading, only a small amount of pore water can flow back into the soil sample. Therefore, the plastic strain during the quiescent period cannot be recovered and remains essentially unchanged.

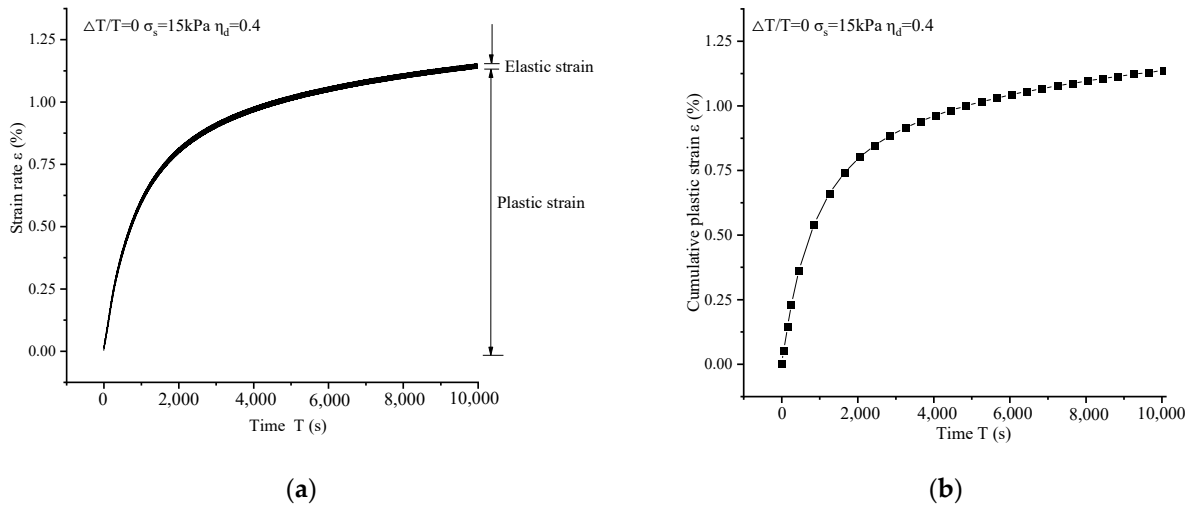


Figure 4. Strain–time curve of dynamic strain under continuous loading conditions. (a) Strain development curve; (b) cumulative strain development curve.

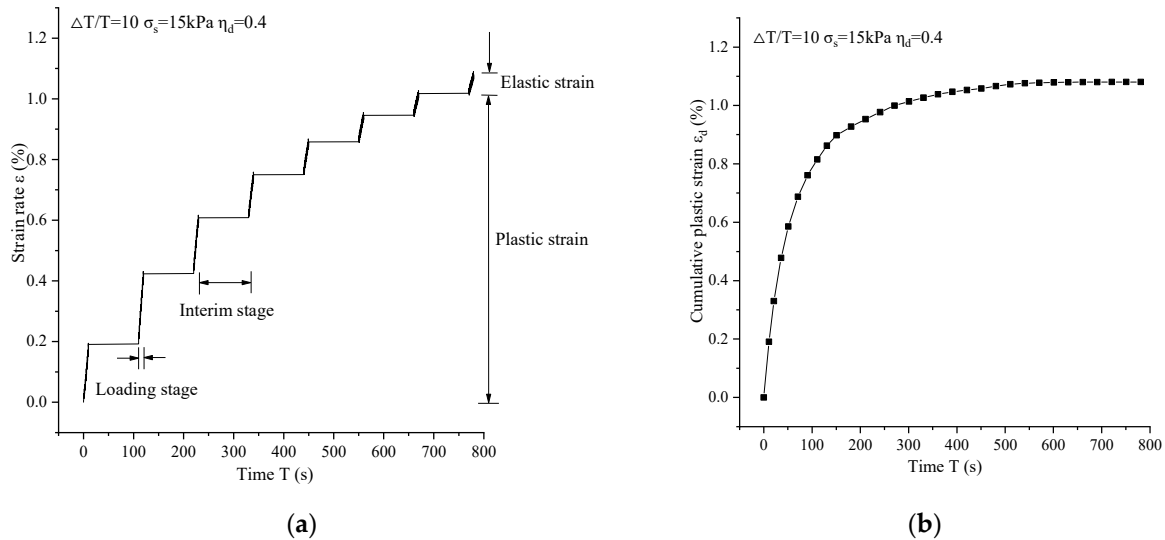


Figure 5. Strain–time curve of dynamic strain under intermittent loading conditions. (a) Strain development curve; (b) cumulative strain development curve.

The development curves of accumulated plastic strain under continuous and intermittent loading conditions are depicted in Figures 4b and 5b, respectively. With the increase in time, the development rate of the strain changes from fast to slow, and the dynamic strain still has an upward trend under the condition of continuous loading at the end, but the dynamic strain gradually approaches the stable value under the condition of intermittent loading. Moreover, it can be observed from the figures that the initial development rate of the plastic strain is significantly higher under intermittent loading conditions. The main reason for this phenomenon is that the accumulation of the strain under continuous

loading conditions depends on the sustained action of external loads. As the number of loading cycles increases, the strain also increases accordingly. However, when the number of loading cycles reaches a certain threshold, the growth rate of the strain begins to decrease. Nevertheless, due to the sustained action of the subway load, the strain does not tend to stabilize until the test termination condition is reached, resulting in a continued upward trend. Under intermittent loading conditions, the dynamic strain is composed of two parts: the deformation induced by the external load during the loading stage and the deformation resulting from the volume reduction caused by pore water expulsion. The volume reduction caused by the release of pore water accounts for the majority of the effect. Thus, it can be inferred that the accumulation rate of plastic strain is initially lower under continuous loading conditions due to the undrained condition. As time progresses, the drainage volume gradually decreases, and the difference in strain between adjacent cycles also decreases. As a result, the development rate of accumulated plastic strain gradually decreases, and the rate of decrease in the development of accumulated plastic strain is faster under intermittent loading conditions compared to continuous loading conditions. Therefore, the accumulated plastic strain ultimately tends to stabilize under intermittent loading conditions.

3.2. Analysis of Accumulated Plastic Strain Behavior of Expansive Soil under Intermittent Loading

3.2.1. Analysis of the Influence of Intermittent Loading Ratio on the Accumulated Plastic Strain

Figure 6 shows the development curve of accumulated plastic strain with the number of cycles under different intermittent loading ratios. Under other conditions, including the same cyclic stress ratio and static deviatoric stress, the evolution of accumulated plastic strain under intermittent loading conditions follows a similar pattern. Initially, during the early stage of cyclic loading, the accumulated plastic strain increases rapidly with the number of vibration cycles. After a certain number of loading cycles, the rate of development curve of the accumulated plastic strain begins to slow down, and the slope of the curve decreases as the number of vibration cycles increases. Eventually, the cumulative plastic strain approaches a stable value.

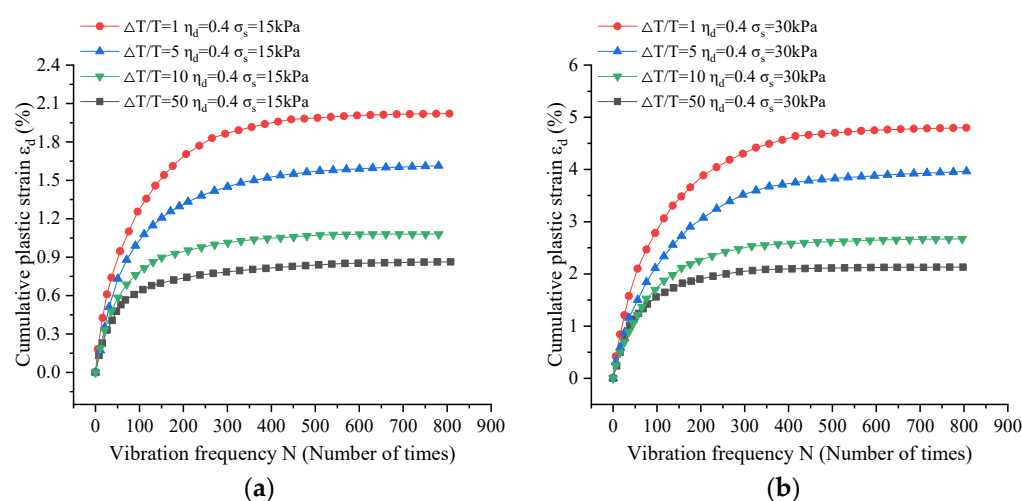


Figure 6. Development curve of accumulated plastic strain with the number of cycles under different stress ratios of intermittent loading. (Sample numbers are S9, S12, S15, S18, S21, S24, S27, S30). (a) $\eta_d = 0.4$ $\sigma_s = 15$ kPa; (b) $\eta_d = 0.4$ $\sigma_s = 30$ kPa.

However, it can be seen from Figure 6a,b that under the same number of cycles, the accumulated plastic strain decreases with the increase in the intermittent loading ratio. This is mainly because, for saturated soil samples, although the dissipation of pore pressure can promote strain growth, the amount of pore pressure dissipation does not continuously increase. Instead, it gradually diminishes over time. With the increase in the intermittent

duration, the growth of accumulated plastic strain no longer depends on the strain growth transformed by the dissipation of pore pressure. At this time, because the recovery of strain when the loading is stopped accounts for the main part, the accumulated plastic strain will ultimately decrease with the increase in the intermittent loading ratio.

3.2.2. Analysis of the Influence Law of Static Deviatoric Stress on the Accumulated Plastic Strain

When the cyclic stress ratio η_d is 0.2, the development law of static deviatoric stress on accumulated plastic strain under intermittent cyclic loading in subway tunnels with $\sigma_s = 15$ kPa and $\sigma_s = 30$ kPa is analyzed as shown in Figure 7. The following conclusions can be drawn from the graph:

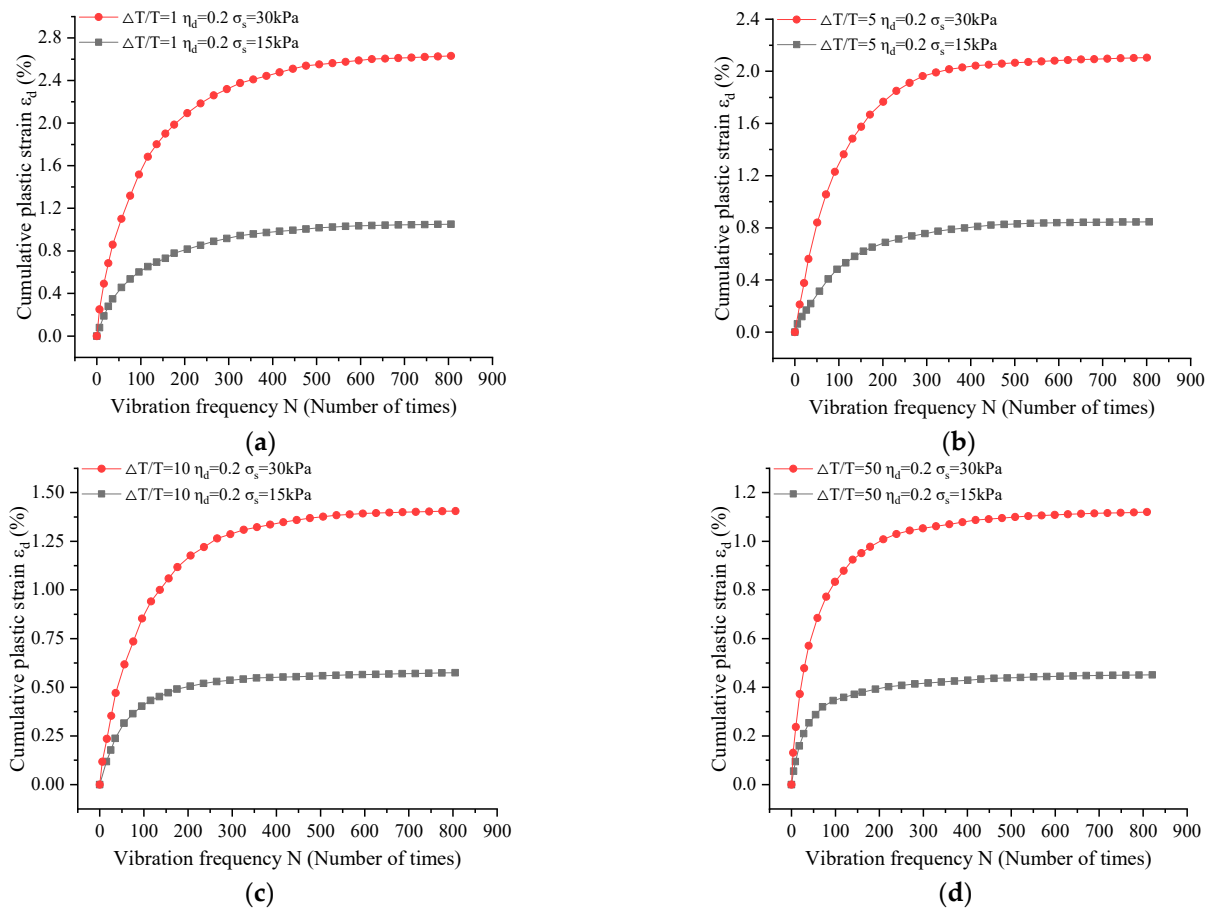


Figure 7. Translation: Development curve of accumulated plastic strain with the number of cycles under different levels of static deviatoric stress. (Sample numbers are S8, S11, S14, S17, S20, S23, S26, S29). (a) $\Delta T/T = 1$; (b) $\Delta T/T = 5$; (c) $\Delta T/T = 10$; (d) $\Delta T/T = 50$.

The accumulation of plastic strain development curves under two different static deviatoric stresses exhibited a similar pattern. Both displayed rapid initial growth followed by a deceleration in growth rate, ultimately reaching a stabilized state. Under the same cyclic loading ratio conditions, it was observed that static deviatoric stress notably influenced the accumulation of strain. The accumulated plastic strain increased with higher static deviatoric stress, leading to conclusions analogous to those from continuous loading scenarios. When the cyclic loading ratio $\Delta T/T$ was 1, the accumulated plastic strain at the point of stabilization under $\sigma_s = 30$ kPa conditions was approximately 150% higher compared to $\sigma_s = 15$ kPa conditions. For cyclic loading ratios of $\Delta T/T$ equal to 5, 10, and 50, the accumulated plastic strain increased by about 150%, 150%, and 149%, respectively. Consequently, doubling the static deviatoric stress resulted in an approximate 150% expansion.

sion in accumulated plastic strain under intermittent subway cyclic loading. Furthermore, the initial strain rate during cyclic loading was also influenced by the magnitude of static deviatoric stress. Larger static deviatoric stress led to higher initial strain rates.

This behavior primarily stems from the structural characteristics of the soil, characterized by weak inter-particle connections and significant instability. In dynamic triaxial testing, the soil experiences the combined effects of cyclic dynamic loading and static deviatoric stress. The substantial external loads lead to instantaneous rupture of the inter-particle connections, causing significant deformation in the initial stages. Consequently, the strain development rate is highest during this phase. When static deviatoric stress remains constant, the strain development rate diminishes, eventually reaching a stable state with minimal fluctuation within a small strain range as the cyclic cycles progress. With increasing static deviatoric stress, the instantaneous deformation of the soil also becomes more substantial, leading to a higher initial strain development rate. In summary, excessive static deviatoric stress significantly accelerates the sustained growth of soil strain.

3.2.3. Analysis of the Influence of Cyclic Stress Ratio on Accumulated Plastic Strain

Figure 8 shows the relationship curve between accumulated plastic strain and number of cycles under the influence of different cyclic stress ratios. As observed from the graph, under consistent conditions, the strain behavior for varying cyclic stress ratios follows a similar pattern. Specifically, in the early stages of cyclic loading, expansive soil experiences a rapid increase in strain. With an increase in the number of cycles, the strain gradually diminishes, eventually stabilizing its growth. As the cyclic stress ratio increases, the strain magnitude for the same number of cycles also increases. Towards the end of the loading process, when the strain development curve approaches stability, the accumulated plastic strain for a cyclic stress ratio of $\eta_d = 0.2$ is approximately 2.8 times that of a cyclic stress ratio of $\eta_d = 0.1$; similarly, for a cyclic stress ratio of $\eta_d = 0.4$, the accumulated plastic strain is roughly 5.4 times that of a cyclic stress ratio of $\eta_d = 0.1$. This demonstrates that an elevated cyclic stress ratio significantly promotes strain development.

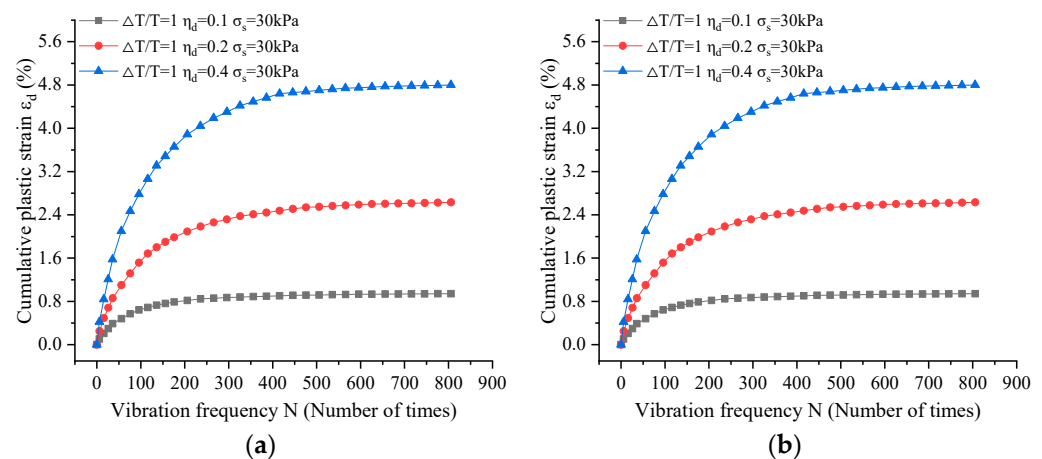


Figure 8. Development curves of accumulated plastic strain with number of cycles under different cyclic stress ratios. (The sample numbers are S10, S11, S12, S22, S23, S24). (a) $\Delta T/T = 1$ $\sigma_s = 30$ kPa; (b) $\Delta T/T = 10$ $\sigma_s = 30$ kPa.

This phenomenon is primarily due to the considerable influence of cyclic dynamic loading on soil deformation. Under smaller loads, the soil experiences elastic deformation without generating plastic strain. However, as external loads increase progressively, plastic strain accumulates within the soil. Consequently, an increase in the cyclic stress ratio leads to a noticeable rise in strain. In comparison to the effect of static bias stress, it is evident that a higher cyclic stress ratio has a slightly greater influence on promoting strain accumulation.

Additionally, it is evident from the graph that at lower cycles, the slope of strain at any given point increases with higher cyclic stress ratios. This can be attributed to the immediate surge in strain caused by initial instantaneous loading. Moreover, the cycles required for the accumulated plastic strain development curve to transition from rapid growth to gradual growth vary with different cyclic stress ratios. A larger cyclic stress ratio corresponds to a higher number of cycles needed for the strain development curve to enter the gradual growth phase. This trend arises from the fact that larger cyclic stresses make it more challenging for a strain to enter a stable growth phase, hence necessitating a higher number of cycles.

4. Classical Accumulated Plastic Strain Modeling Analysis

Currently, researchers from both domestic and international backgrounds have extensively investigated the accumulation of strain in soils under cyclic loading, and have proposed different strain models based on their research results, which can be summarized as explicit or implicit models related to accumulated plastic strain of soil samples and the number of cycles and experimental parameters. Classical accumulated plastic strain calculation models can roughly be divided into the following two types.

(1) Exponential Model represented by the Monismith Model

The exponential model proposed by Monismith et al. [23] is one of the widely used models, and subsequent scholars mostly used this model as a foundation and made refinements to develop improved models. The formula is expressed as follows:

$$\varepsilon_p = aN^b \quad (1)$$

In the equation: ε_p —accumulated plastic strain; a , b —related test parameters; N —number of cyclic vibrations.

Anand et al. [24] based their research on the Monismith exponential model, and considering factors such as confinement pressure and deviatoric stress, they proposed a modified model.

$$\varepsilon_p = a \left(\frac{\sigma_{oct}}{p_a} \right)^m N^b \quad (2)$$

In the equation: σ_{oct} —shear stress; p_a —atmospheric pressure, with a value of 101 kPa; a , b , m —test parameters; N —number of cyclic vibrations.

Chai et al. [25] developed a model that comprehensively considers the effects of initial static deviatoric stress, dynamic deviatoric stress, and static failure deviatoric stress. The formula is expressed as follows:

$$\varepsilon_p = a \left(\frac{\sigma_d}{\sigma_f} \right)^m \left(1 + \frac{\sigma_{is}}{\sigma_f} \right)^n N^b \quad (3)$$

In the equation: ε_p —accumulated plastic strain; a , b , m , n —test parameters; σ_d , σ_f , σ_{is} —dynamic stress amplitude, static failure deviatoric stress, and initial static deviatoric stress, respectively; N —number of cyclic vibrations.

(2) Tang Yiqun Logit Model

Tang Yiqun [26] proposed using logarithmic relationship curves to reflect the strain accumulation characteristics of reinforced soils around tunnels under Shanghai subway loads. The model comprehensively considers the influences of dynamic stress amplitude, consolidation ratio, confining pressure, and soil properties. The specific calculation model is as follows:

$$\varepsilon_p = A \ln N + B \quad (4)$$

In the equation: ε_p —accumulated plastic strain; A , B —parameters related to influencing factors; N —number of cyclic vibrations.

Fitting of the experimental results was carried out using both the Monismith index model and the Tang Yiqun model. However, due to the congruence of the conclusions drawn from both models, only specimens S8 and S29 were chosen for detailed illustration, with the omission of further elaboration on the remaining samples. This is demonstrated in Figures 9 and 10.

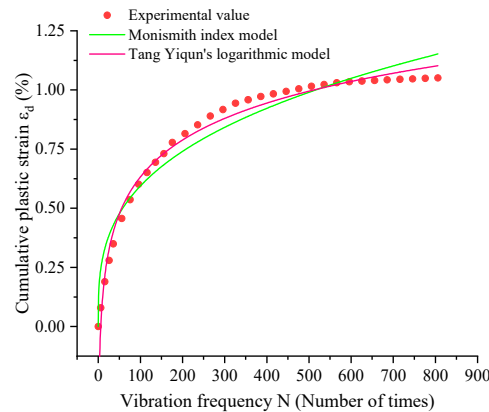


Figure 9. Fitting results of sample S8.

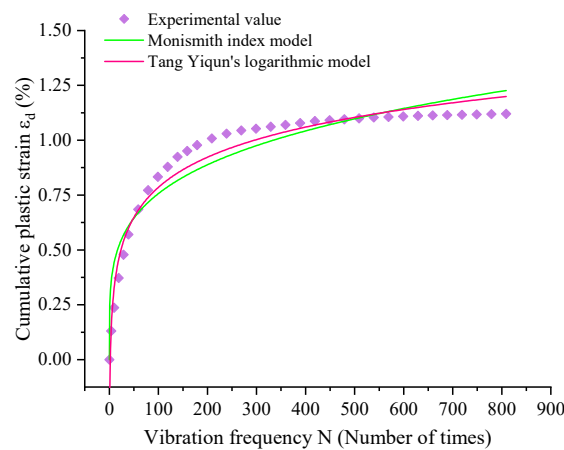


Figure 10. Fitting results of sample S29.

In comparison with the experimental data, prior to the inflection point of the fitting curves, the logarithmic model proposed by Tang Yiqun exhibits closer alignment with the experimental values. However, beyond this inflection point, both fitted curves deviate significantly from the experimental data. Consequently, for lower cycle numbers, Tang Yiqun’s logarithmic model provides a better fit to the experimental data than the Monismith index model. Nevertheless, as the cycle numbers increase, both models continue to exhibit a rising trend, whereas the experimental values in this study tend to stabilize and show incremental growth. Ultimately, it can be determined that neither the Monismith index model nor the Tang Yiqun logarithmic model adequately captures the behavior observed in this study’s experimental results.

5. Establishment of Accumulated Plastic Strain Model

Therefore, the development of accumulated plastic strain under intermittent subway loading is more suitable to be described by the hyperbolic model. The mathematical expression of the relationship between accumulated plastic strain and the number of cycles is shown in the following equation.

$$\epsilon_d = \frac{N}{a + b \cdot N + c\sqrt{N}} \tag{5}$$

In the equation: ϵ_d —accumulated plastic strain; a, b, c —fitted parameters associated with different influencing factors; N —number of cycles.

The strain curve of the soil sample under intermittent loading conditions was fitted, and the fitting effect is shown in Figure 11. The related fitting parameters of the strain calculation model are shown in Table 3. From this analysis, it is evident that the coefficient of determination (R^2) for the specimens is consistently close to 1. A higher R^2 value indicates a stronger fit of the model to the data. As such, the experimental results can be effectively represented using the proposed cumulative plastic strain calculation model.

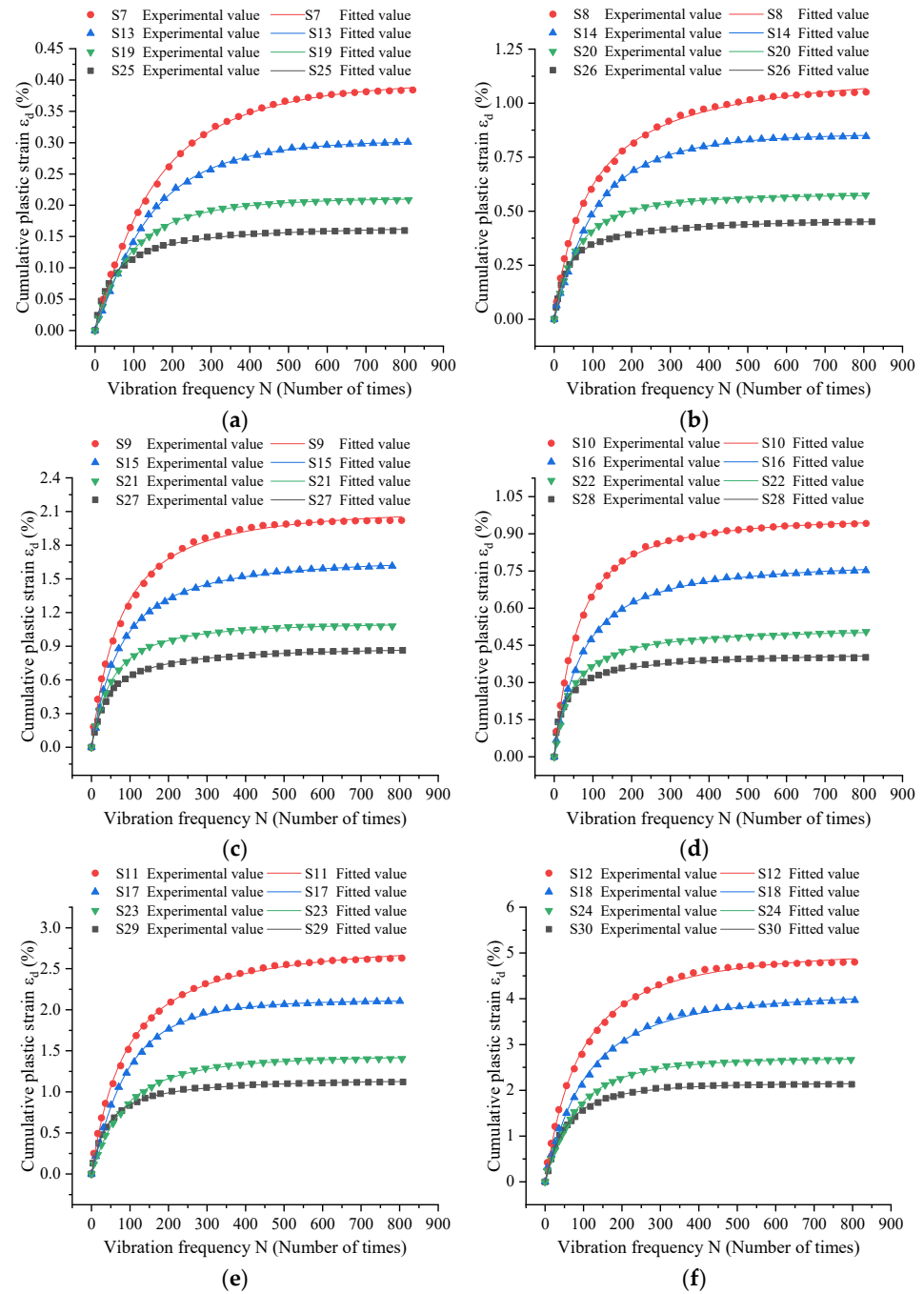


Figure 11. Comparison of test results and fitted values of soil samples under intermittent loading conditions. (a) Soil sample S7, S13, S19, S25; (b) soil sample S8, S14, S20, S26; (c) soil sample S9, S15, S21, S27; (d) soil sample S10, S16, S22, S28; (e) soil sample S11, S17, S23, S29; (f) soil sample S12, S18, S24, S30.

Table 3. Accumulated plastic strain model parameters under intermittent loading conditions.

Soil Sample Number	Fitting Parameter <i>a</i>	Fitting Parameter <i>b</i>	Fitting Parameter <i>c</i>	Correlation Coefficient R ²
S7	0.00182	0.00517	−0.04868	0.99925
S8	0.01350	0.01123	0.00458	0.99887
S9	0.02542	0.01213	−0.02809	0.99766
S10	0.01363	0.02225	−0.0058	0.99926
S11	0.03001	0.01060	−0.01619	0.99878
S12	0.05009	0.01008	−0.02974	0.99837
S13	0.00133	0.00534	−0.06115	0.99972
S14	0.00583	0.00764	−0.05782	0.9994
S15	0.01951	0.0118	−0.02916	0.99958
S16	0.01622	0.01264	−0.0248	0.99946
S17	0.01559	0.00849	−0.06604	0.99952
S18	0.03136	0.00798	−0.03901	0.99825
S19	0.00173	0.00897	−0.05603	0.9996
S20	0.00827	0.01494	−0.04905	0.99979
S21	0.01871	0.01713	−0.03461	0.99978
S22	0.01168	0.02225	−0.0058	0.99926
S23	0.01336	0.00987	−0.04763	0.99919
S24	0.02545	0.0103	−0.05811	0.99913
S25	0.00384	0.02234	0.00511	0.99869
S26	0.01486	0.03105	0.0196	0.99966
S27	0.02068	0.02263	0.00211	0.99929
S28	0.02723	0.06080	0.13971	0.99741
S29	0.02697	0.02311	−0.01206	0.9991
S30	0.03289	0.01593	−0.05258	0.99914

6. Conclusions

Taking the saturated remolded expansive soil in Hefei City as the research object, the dynamic characteristics of the soil under intermittent and continuous subway loading conditions were investigated through cyclic triaxial tests. The research aimed to explore the influence of intermittent and continuous loading modes on the dynamic behavior of saturated remolded expansive soil. The study also analyzed the effects of intermittent loading ratio, cyclic stress ratio, and static deviator stress on the variation of cumulative plastic strain with the number of cycles. Based on the test results, the following conclusions can be drawn:

- (1) Under both intermittent and continuous subway loading, the accumulated plastic strain of saturated remolded expansive soil exhibited a similar development pattern of rapid growth–slow growth–eventual stabilization. It can be inferred that intermittent loading does not alter the overall trend of strain development but does show differences in the initial accumulation rate and final development of plastic strain. Comparative analysis revealed that the initial development rate of accumulated plastic strain was higher under intermittent loading conditions than under continuous loading conditions, and intermittent loading facilitated a quicker stabilization of cumulative plastic strain in the soil.
- (2) Under intermittent subway loading with other test conditions being the same, a larger intermittent loading ratio resulted in smaller accumulated plastic strain at the same number of cycles, and the accumulated plastic strain value at stabilization was also smaller. Static deviatoric stress and cyclic stress ratio have a significant cumulative effect on plastic strain. When static deviatoric stress increases by one time, the accumulated plastic strain under intermittent subway cyclic loading increases by about 1.5 times. When the cyclic stress ratio increases by one time, the accumulated plastic strain increases by about 1~2 times.
- (3) Based on the cumulative plastic strain development behavior under intermittent subway cyclic loading, an enhanced calculation model for cumulative plastic strain as a function of cycle count was proposed, building upon the Long–Yao hyperbolic

model. This model takes into account factors such as intermittent loading ratio, static bias stress, and cyclic stress ratio. The coefficient of determination (R^2) for this model is remarkably close to 1, affirming its high degree of fitness to the data. As a result, the proposed model demonstrates a notably favorable fitting performance.

Author Contributions: Writing—original draft, L.Z.; Writing—review & editing, Y.G., G.C. and X.L. All authors have read and agreed to the published version of the manuscript.

Funding: This research was funded by [2020 Natural Science Foundation of Anhui Province] grant number [2008085ME168] and by [2021 Project on Cultivation of Outstanding Top Talents in Universities].

Institutional Review Board Statement: Not applicable.

Informed Consent Statement: Not applicable.

Data Availability Statement: Not applicable.

Conflicts of Interest: The authors declare no conflict of interest.

References

1. Yang, H.; Qu, Y.; Zheng, J.; Liu, L. Preliminary Study on Engineering Geological Problems of Expansive Soil in Highway Construction in Western China. *J. Chang. Commun. Univ.* **2003**, *19*, 19–24.
2. Xie, Y.; Chen, Z.; Li, G. Study on law of three-dimensional expansive force of expansive soil in Nanyang. *J. Logist. Eng. Coll.* **2006**, *11–14*+23.
3. Xu, Y.; Cheng, Y.; Xiao, J.; Lin, Y.; Qi, S. Research on Expansive Soil Landslide and New Prevention Technology for Engineering Slope. *J. Geotech. Eng.* **2022**, *44*, 1281–1294.
4. Liu, Q.; Xiang, W.; Wu, Y. *Study on Engineering Characteristics and Modification Theory of Expansive Soil*; China University of Geosciences Press: Wuhan, China, 2015; pp. 1–99.
5. Liao, S. *Expansive Soil and Railway Engineering*; China Railway Publishing House: Beijing, China, 1984; pp. 1–214.
6. Chen, S. *Research on Engineering Characteristics and Treatment Technology of Expansive Soil*; Huazhong University of Science and Technology: Wuhan, China, 2006.
7. Tang, X.; Wang, S.; Cheng, F. Experimental study on dynamic stress dynamic strain relationship and dynamic modulus of reinforced expansive soil. *IOP Conf. Ser. Earth Environ. Sci.* **2021**, *669*, 012006. [[CrossRef](#)]
8. Yang, Z.; Zhang, L.; Ling, X.; Li, G.; Tu, Z.; Shi, W. Experimental study on the dynamic behavior of expansive soil in slopes under freeze-thaw cycles. *Cold Reg. Sci. Technol.* **2019**, *163*, 27–33. [[CrossRef](#)]
9. Chen, H. *Experimental Study on Dynamic Characteristics of Expansive Soil under Cyclic Loading*; Hefei University of Technology: Hefei, China, 2021.
10. Zhuang, X. Experimental Study on Cumulative Deformation and Dynamic Strength Characteristics of Weak Expansive Soil under Cyclic Loading. *Geotech. Mech.* **2020**, *41*.
11. *GB/T50123-2019*; Standard Test Methods for Geotechnical Investigation. GB Standards: Taiwan, China, 2019.
12. *GB 50911-2013*; Technical Specification for Monitoring of Urban Rail Transit Project. GB Standards: Taiwan, China, 2013.
13. Zheng, Q.; Xia, T.; Zhang, M. Strain prediction model of intact silty clay under intermittent cyclic loading. *J. Zhejiang Univ.* **2020**, *54*, 889–898.
14. Wen, R.; Wang, C.; Chen, Y. Influence of static uniaxial stress caused by traffic load on deformation of saturated soft clay. *Rock Soil Mech.* **2009**, *30* (Suppl. S2), 119–122.
15. Chen, C.; Zhou, Z.; Zhang, X. Experimental study on dynamic cumulative characteristics of peat soil under cyclic loading. *Chin. J. Rock Mech. Eng.* **2017**, *36*, 1247–1255.
16. Wang, R.; Wang, L.; Hu, Z.; Zhao, Z.; Li, X.; Wang, Q. Influence of static uniaxial stress caused by traffic load on dynamic characteristics of compacted loess. *J. China Railw. Soc.* **2019**, *41*, 110–117.
17. Wang, Y. *Research on Dynamic Stability of Subway Tunnel-Soil under Cyclic Loading*; Tongji University: Shanghai, China, 2002.
18. Chen, X.; Nie, R.; Li, Y.; Guo, Y.; Dong, J. Resilient modulus of fine-grained subgrade soil considering load interval: An experimental study. *Soil Dyn. Earthq. Eng.* **2021**, *142*, 106558. [[CrossRef](#)]
19. Zhang, Y.; Bai, B. Simulation of excitation load of tunnel structure induced by subway train vibration. *J. Vib. Shock.* **2000**, *3*, 70–72+78+96.
20. Lei, S.; Hui, H. Comparative analysis of static and dynamic characteristics of expansive soil and its improved soil. *Chin. J. Rock Mech. Eng.* **2004**, *23*, 3003–3008.
21. Zhou, X. *Study on Dynamic Characteristics and Subgrade Response of Expansive Soil under Bi-Directional Cyclic Load*; Institute of Rock and Soil Mechanics, Graduate University of Chinese Academy of Sciences: Wuhan, China, 2010.
22. Zhuang, J. *Study on Dynamic Characteristics and Micro-Experimental of Soft Clay under Metro Circulatory Loads*; Zhejiang University: Hangzhou, China, 2019.

23. Monismith, C.L.; Ogawa, N.; Freeme, C.R. Permanent deformation characteristics of subgrade soils due to repeated loading. *Transp. Res. Rec.* **1975**, *537*, 1–17.
24. Anand, J.P.; Louay, N.M.; Aaron, A. Permanent deformation characterization of subgrade soils form RLT test. *J. Mater. Civ. Eng.* **1999**, *11*, 274–282.
25. Chai, J.; Miura, N. Traffic-Load-Induced Permanent Deformation of Road on Soft Subsoil. *J. Geotech. Geo-Environ. Eng.* **2002**, *128*, 907–916. [[CrossRef](#)]
26. Tang, Y.; Zhao, H.; Wang, Y.; Liu, R. Strain accumulation characteristics of surrounding soft clay reinforced under subway load. *J. Tongji Univ.* **2011**, *39*, 972–977.

Disclaimer/Publisher’s Note: The statements, opinions and data contained in all publications are solely those of the individual author(s) and contributor(s) and not of MDPI and/or the editor(s). MDPI and/or the editor(s) disclaim responsibility for any injury to people or property resulting from any ideas, methods, instructions or products referred to in the content.